

Thermal cure kinetics of epoxidized linseed oil with anhydride hardener

Arunjunai Raj Mahendran · Günter Wuzella ·
Andreas Kandelbauer · Nicolai Aust

Received: 9 March 2011 / Accepted: 8 April 2011 / Published online: 23 April 2011
© Akadémiai Kiadó, Budapest, Hungary 2011

Abstract The thermal cure kinetics of an epoxidized linseed oil with methyl nadic anhydride as curing agent and 1-methyl imidazole as catalyst was studied by differential scanning calorimetry (DSC). The curing process was evaluated by non-isothermal DSC measurements; three iso-conversional methods for kinetic analysis of the original thermo-chemical data were applied to calculate the changes in apparent activation energy in dependence of conversion during the cross-linking reaction. All three iso-conversional methods provided consistent activation energy versus time profiles for the complex curing process. The accuracy and predictive power of the kinetic methods were evaluated by isothermal DSC measurements performed at temperatures above the glass transition temperature of the completely cured mixture ($T_{g\infty}$). It was found that the predictions obtained from the iso-conversional method by Vyazovkin yielded the best agreement with the experimental values. The corresponding activation energy (E_a) regime showed an increase in E_a at the beginning of the curing which was

followed by a continuous decrease as the cross-linking proceeded. This decrease in E_a is explained by a diffusion controlled reaction kinetics which is caused by two phenomena, gelation and vitrification. Gelation during curing of the epoxidized linseed/methyl nadic anhydride system was characterized by rheological measurements using a plate/plate rheometer and vitrification of the system was confirmed experimentally by detecting a significant decrease in complex heat capacity using alternating differential scanning calorimetry (ADSC) measurements.

Keywords Epoxidized linseed oil · Thermal cure kinetics · Model-free kinetic methods · Iso-conversional methods · Diffusion controlled kinetics · Vitrification · Alternating differential scanning calorimetry

Introduction

Vegetable oils are currently mainly used in the food industry and for the production of bio-diesel [1], detergents [2], lubricants [3], paints, and cosmetics [4]. Due to environmental problems and increasingly restricted availability of non-renewable, fossil-based products, vegetable oils being bio-renewable resources are frequently chemically modified for further use as renewable biopolymers and resin matrices for bio-composites. Oxygen insertion via epoxidation of the unsaturated double-bonds of natural oils transforms the triglycerides into reactive oxiran moieties which are capable of further cross-linking via ring-opening reactions [5–8]. The preparation of such bio-based epoxy resins from epoxidized natural oils has been studied already by several authors [9–14]. The epoxidized oils are mainly cured with cyclic acid anhydrides and used as matrices for composites [15, 16]. Apart from other

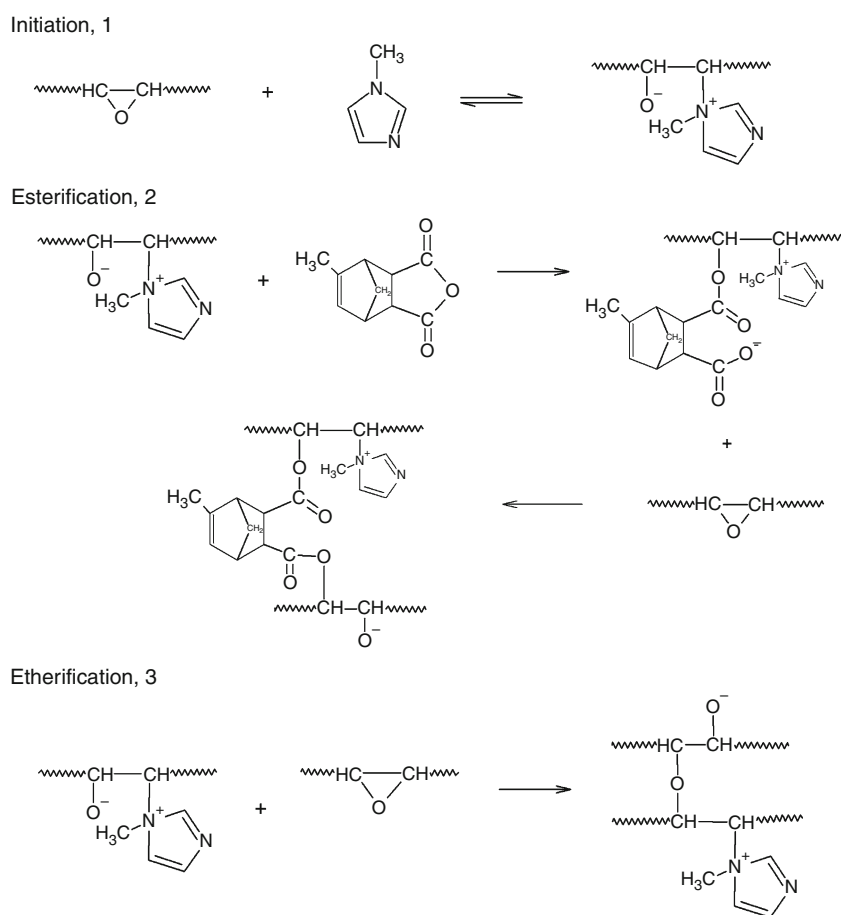
A. R. Mahendran · G. Wuzella
WOOD Carinthian Competence Center (W3C),
Kompetenzzentrum Holz GmbH, Klagenfurterstrasse 87-89,
9300 St. Veit an der Glan, Austria

A. Kandelbauer (✉)
School of Applied Chemistry, Reutlingen University,
Alteburgstrasse 150, 72762 Reutlingen, Germany
e-mail: andreas.kandelbauer@reutlingen-university.de

A. Kandelbauer
Department of Wood Science and Technology, University
of Natural Resources and Life Sciences, Peter Jordan Strasse 82,
1190 Vienna, Austria

N. Aust
Department of Chemistry of Polymeric Materials, University
of Leoben, Otto-Glöckel-Straße 2, 8700 Leoben, Austria

Scheme 1 Reaction scheme for the polymerization of epoxidized linseed oil using imidazole as an initiator and nadic methyl anhydride as a cross-linker, (1) initiation, (2) esterification, and (3) etherification



anhydride hardeners, methyl-5-norbornene-2,3-dicarboxylic anhydride or nadic methyl anhydride (NMA) was used as a cross-linking agent; since it is liquid at room temperature it can easily be mixed with the resin and the final cured network possesses a very high heat distortion temperature [17]. The curing of thermo-setting resins is generally rather complex due to the interaction between chemical kinetics and the simultaneous changes in their physical properties and the development of mechanical properties of the solid material [18].

The initial curing stage of epoxidized linseed oil typically follows a chemically controlled reaction mechanism. Imidazole initiates the curing reaction by opening the oxiran ring under formation of a zwitterion [19] (Scheme 1, 1). The subsequent cross-linking of the modified linseed oil can proceed via two principal pathways: esterification and etherification [20]. The reaction of the alkoxide anion at the epoxy backbone with an anhydride molecule leads to formation of a monoester, which in turn may react with an epoxy group to give a diester (esterification mechanism, Scheme 1, 2). Alternatively, the alkoxide anion may directly attack an epoxy functional group which results in an ether linkage that may undergo further cross-linking. According to Park and his co-workers [13], the etherification of epoxy

groups with alkoxides is much slower than the esterification reaction with anhydrides or carboxylates and hence, reaction 2 (Scheme 1) can safely be assumed to be the dominant reaction in the present epoxy-imidazole system [21].

Etherification and esterification take place in parallel to different extents and their varying relative contributions to the overall net cross-linking reaction can lead to time- (or, conversion-) dependent variations in the overall apparent activation energy during the curing of the epoxy-anhydride system as determined by model-free kinetic thermo-analytical methods. Two important phase transitions occur during curing, namely, gelation and vitrification. Gelation is the incipient formation of a cross-linked network, and it is a most distinguishing characteristic of a thermo-set. Gelation does not usually inhibit the process of curing, and it cannot be detected by techniques which are sensitive only to the chemical reaction. The most sophisticated method for the determination of gelation is rheology [22]. Vitrification is another phenomenon, which may or may not occur during curing depending on the selected curing temperature relative to the glass transition temperature T_g of the fully cured network. During cure the T_g is increasing until it reaches the highest possible glass transition temperature which is the glass transition temperature of the

fully cured network ($T_{g\infty}$). When T_g reaches the selected cure temperature the system vitrifies. Hence vitrification can be avoided by applying curing temperatures at or above $T_{g\infty}$. In the case of isothermal curing conditions, vitrification occurs once the glass transition temperature equals the curing temperature whereas in the case of curing under non-isothermal conditions, vitrification takes place when the increasing glass transition temperature reaches the actual curing temperature. If vitrification occurs, then the reaction rate will undergo a significant decrease and fall well below the chemical reaction rate, which means that the reaction becomes controlled by the diffusion of the reactants [23]. This chemo-rheological transition can be followed simultaneously with the reaction rate in alternating differential scanning calorimetry (ADSC) [24].

Bio-resins are currently replacing many resins derived from non-renewable resources in the composites and automobile industries. Hence, detailed knowledge on the cure kinetics of such systems is becoming increasingly important, especially when it leads to reliable predictions of the end-use properties of the cured network.

Kinetics of epoxy curing with anhydride hardener was studied by numerous authors [25–27] who generally based their calculations of rate constants on the fitting of reaction models. Since such model-based fitting methods consider only single averaged values of activation energy which are assumed to be constant throughout the whole course of the cross-linking reactions, they tend to produce highly uncertain kinetic predictions for rather complex cure mechanisms. Model-free (or iso-conversional) kinetic methods on the other hand rely on conversion-dependent, non-constant apparent activation energy and therefore are likely to produce more consistent kinetics results from isothermal and non-isothermal experiments [28]. Especially with complex reaction mixtures such as the present epoxidized linseed oil–imidazole–anhydride system, model-free kinetic approaches may prove superior to model-based ones since quantitative knowledge on the reaction mechanism is not known and the system in question is not forced within the restrictions of uncertain mechanistic assumptions.

The cure kinetics of this renewable resin has not been analyzed by model-free kinetic methods before and the characterization of the physical phenomena during cure using rheology and ADSC of this system has yet not been reported. Hence, in this article, the cure kinetics of this system was studied using three different model free kinetic methods, the predictive power of the various approaches was compared and the development of mechanical properties as well as the gelation and vitrification behavior of the cross-linking bio-resin were analyzed by thermal and rheological methods. The theory behind model free kinetic analysis is briefly summarized in the next section.

Theory of thermoanalytical methods

Theory of isoconversional kinetic analysis

All mathematical approaches to describe the temperature dependence of the reaction rate for a specific chemical reaction are based on the fundamental rate equation [29]:

$$\frac{d\alpha}{dt} = A \exp\left(\frac{-E}{RT}\right) f(\alpha) \quad (1)$$

where t is the time (s), T the temperature (K), α the Conversion (0–1), $f(\alpha)$ the reaction model, R the gas constant ($8.314 \text{ J mol}^{-1} \text{ K}^{-1}$), E the activation energy (kJ mol^{-1}), and A is the pre-exponential factor (s^{-1}).

From the integral of a dynamic DSC thermogram, both conversion, α , and the change of conversion with time, $\alpha(t) = d\alpha/dt$, are determined at a specific cure time (t). The $\alpha(t)$ value is determined from dynamic runs as the ratio between the heat released until time t and the total heat of the reaction according to Eqs. 2 and 3:

$$\alpha(t) = (\Delta H_p)_t / \Delta H_0 \quad (2)$$

$$d\alpha(t)/dt = (dH/dt) / \Delta H_0 \quad (3)$$

Integration of the enthalpy curve from t_0 to t yields the degree of conversion $\alpha(t)$ for any time t between t_0 and t_∞ as the ratio $H_{t_0\dots t}/H_\infty$ where H_∞ is the integral of the enthalpy curve from t_0 to t_∞ and $H_{t_0\dots t}$ is the integral of the enthalpy curve from t_0 to t [15]. The differential $d\alpha/dt$ for each time t between t_0 and t_∞ was calculated as H_t/H_∞ where H_t is the current measured enthalpy at time t .

Based on the Arrhenius equation (1), the progress of a chemical reaction is described by three kinetic parameters, the pre-exponential factor, A , the activation energy, E , and the reaction model, $f(\alpha)$. Classical kinetic analysis requires a priori knowledge on the reaction mechanism and hence is model-dependent. The reaction model $f(\alpha)$ may take various forms based on different types of reactions or processes (phase boundary reaction, diffusion, chemical reaction, nucleation, nucleus growth). However, the curing of thermosetting resins such as the chemically modified linseed oil mixture investigated in the present study is rather a complex multi-step process than a simple chemical reaction of quantitatively known mechanism [8]. Hence, classical model-dependent kinetic analysis is not suitable to predict cure kinetics for the exact reaction model is usually unknown. For complex processes model-free kinetics or so-called iso-conversional methods have been developed which assume that the effective activation energy at a particular degree of cure, α , is independent of the temperature program (iso-conversional principle). Multiple studies [23, 30] have been performed already for complex thermoset curing mechanisms using the iso-conversional

principle which impressively illustrate the potential of MFK approaches for the understanding of complex cross-linking reactions. The methods can be divided into differential and integral methods. In the current work, the differential method of Friedman (FR) [31] and the integral methods of Kissinger–Akahira–Sunose (KAS) [32, 33] and Vyazovkin in its advanced form (VA) [34, 35], were used to predict the dependence of the effective activation energy on the degree of cure, $E(\alpha)$, for the resin mixture of an epoxidized linseed oil with methyl nadic anhydride as curing agent and 1-methyl imidazole as catalyst. The theory behind model-free kinetic approaches, starting from basic rate equations to the prediction of activation energy using different models are discussed in more detail in several recently published papers [34–37].

From the three calculated activation energy curves, $E(\alpha)$, and the dynamic DSC data of any heating rate β the time (t_x) required for a certain degree of cure at an arbitrary isothermal temperature T_0 can be estimated using the following formula [38]:

$$t_x = \frac{\int_0^{T_x} \exp\left(\frac{-E_x}{RT}\right) dT}{\beta \exp\left(\frac{-E_x}{RT_0}\right)} \quad (4)$$

Alternating differential scanning calorimetry

Differential scanning calorimetry with modulated temperature signal is the principal of ADSC which provides some beneficial information for the thermal characterization of the polymeric materials. The simultaneous measurement of heat capacity, heat flow, and the phase angle between heat flow and heating rate enables a more detailed study of the polymer systems both in isothermal or quasi isothermal and non-isothermal conditions. ADSC is based on the temperature modulation during a constant heating rate in the non-isothermal experiments:

$$T = T_0 + q_0 t + A_T \sin(\omega)t \quad (5)$$

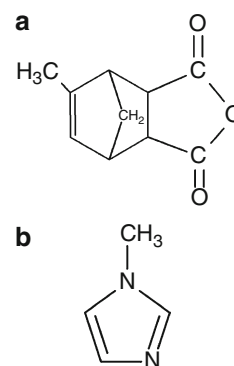
where $\omega = 2\pi/t_p$, $T(t)$ is the temperature as a function of time, T_0 the initial temperature ($^{\circ}\text{C}$), q_0 the underlying heating rate ($^{\circ}\text{C min}^{-1}$), t_p the period (min), ω the angular frequency, A_T the amplitude ($^{\circ}\text{C}$).

The detailed theory and calculation of complex heat capacity, reversing and non-reversing heat flow are discussed elsewhere [39–42].

Experimental

The bio-based resin used in the present study was a commercial epoxidized linseed oil supplied by Cognis GmbH, Düsseldorf (Dehysol B 316 having Acid value 0.43 KOH/g,

Fig. 1 Chemical structures of methyl-5-norbornene-2,3-dicarboxylic anhydride (nadic anhydride) (a), 1-methyl imidazole (b)



iodine value 3.0 g I₂/100 g). It was cured with hardener, methyl-5-norbornene-2,3-dicarboxylic anhydride (NMA) purchased from Sigma–Aldrich, in the presence of 1-methyl imidazole initiator from Sigma–Aldrich. The chemical structures of the reactants are shown in Fig. 1.

The epoxidized linseed oil (ELO) was mixed with NMA in stoichiometric amounts (anhydride equivalent/epoxy equivalent) and the mixing proportion along with 1-methyl imidazole (1-MI) was ELO:NMA:1-MI = 100:80:1.8.

The DSC measurements were performed by a METTLER TOLEDO 822e instrument (Greifensee, Switzerland) and STAR[®] software was used for the evaluation of the DSC curves. The linseed oil was mixed well with the reagents at room temperature and for each experiment approximately 5–6 mg of the mixture was weighed in the hermetic aluminium DSC pan. The pan was sealed by crimping and heated from 25 to 300 $^{\circ}\text{C}$ at three different scanning rates 10, 15 and 20 $^{\circ}\text{C min}^{-1}$ in a nitrogen atmosphere. Kinetic analysis according to the model-free approaches by FR and KAS were performed with the computer program Excel. For kinetic analysis according to the VA method, the STAR[®] software package from Mettler Toledo (Greifensee, Switzerland) was used.

The ADSC measurements were performed in the same DSC instrument. The non-isothermal ADSC experiments were done at heating rates of 1 $^{\circ}\text{C min}^{-1}$ with an amplitude of modulation of 0.5 $^{\circ}\text{C}$ for 60 s to calculate the heat capacity (in J g⁻¹ K⁻¹) as a function of temperature. In a second heating run of the fully cured sample under otherwise same conditions the heat capacity of the fully cured network was determined. The glass transition temperature of the fully cured epoxy resin was determined from the traces of heat capacities, phase angle and heat flow signals obtained at an underlying heating rate of 1 $^{\circ}\text{C min}^{-1}$ and a modulation of 0.5 $^{\circ}\text{C}$ and 60 s. The temperature range considered for all ADSC measurements was between 100 and 220 $^{\circ}\text{C}$, because within this temperature range the curing reaction occurs. The dynamic glass transition temperature $T_{g\infty}$ was determined at the midpoint of the variation in the modulus of the complex heat capacity [42].

The rheological behavior of the resin during curing was characterized using Physica MCR 101 Rheometer from Anton Paar GmbH (Graz, Austria). Dynamic temperature sweep measurements were carried out with parallel plate geometry using a linear temperature program at a heating rate of $10\text{ }^{\circ}\text{C min}^{-1}$ ranging from 25 to $180\text{ }^{\circ}\text{C}$ with an angular frequency of 10 s^{-1} and a constant deformation of 10%. The complex viscosity (in Pa s), the storage modulus G' (in Pa) and the loss modulus G'' (in Pa) were recorded versus time and temperature, respectively. To characterize the transition from the sol- to the gel-state (gelation) the temperature at which the storage modulus G' intersects the loss modulus G'' was determined.

Results and discussion

Alternating differential scanning calorimetry analysis

The total heat flow signal shows an exothermic peak which is characteristic for the curing reaction. The total enthalpy measured by dynamic DSC ($\Delta H = 64\text{ J g}^{-1}$) was almost identical to the curing heat flow as measured in the ADSC experiment (63 J g^{-1}). The complex heat capacity, total heat flow signal, and the degree of cure with respect to temperature are shown in Fig. 2. In Fig. 2, the complex

heat capacity starts to decrease at around $120\text{ }^{\circ}\text{C}$ until a temperature of $160\text{ }^{\circ}\text{C}$ is reached. At temperatures above $160\text{ }^{\circ}\text{C}$ the complex heat capacity increases again. The significant decrease of complex heat capacity is indicative of vitrification at low heating rate ($1\text{ }^{\circ}\text{C/min}$) and the subsequent increase corresponds to a devitrification process. As soon as vitrification occurs, the kinetics of curing becomes diffusion controlled.

Another ADSC measurement of the fully cured epoxidized linseed oil was made to determine $T_{g\infty}$ calculated at the midpoint of the variation in the modulus of the complex heat capacity. The $T_{g\infty}$ for the current curing system is $176\text{ }^{\circ}\text{C}$ (Fig. 3). According to Montserrat et al. [43], as the heating rate under non-isothermal curing conditions is increased, the time interval during which the system remains in a glassy state becomes shorter until the phenomenon of vitrification is totally avoided. If on the other hand under isothermal curing conditions the selected curing temperature is chosen high enough, the glass transition temperature T_g of the system remains always below the curing temperature and the system does not reach the glassy state at all [43]. Hence, the high glass transition temperature of the epoxy system studied confirms that there is the risk of vitrification in case of very low heating rates for non-isothermal curing (Fig. 2) and at isothermal process temperatures below the $T_{g\infty}$, respectively.

Fig. 2 Degree of cure, complex heat capacity, and total heat flow curves for the epoxidized linseed oil

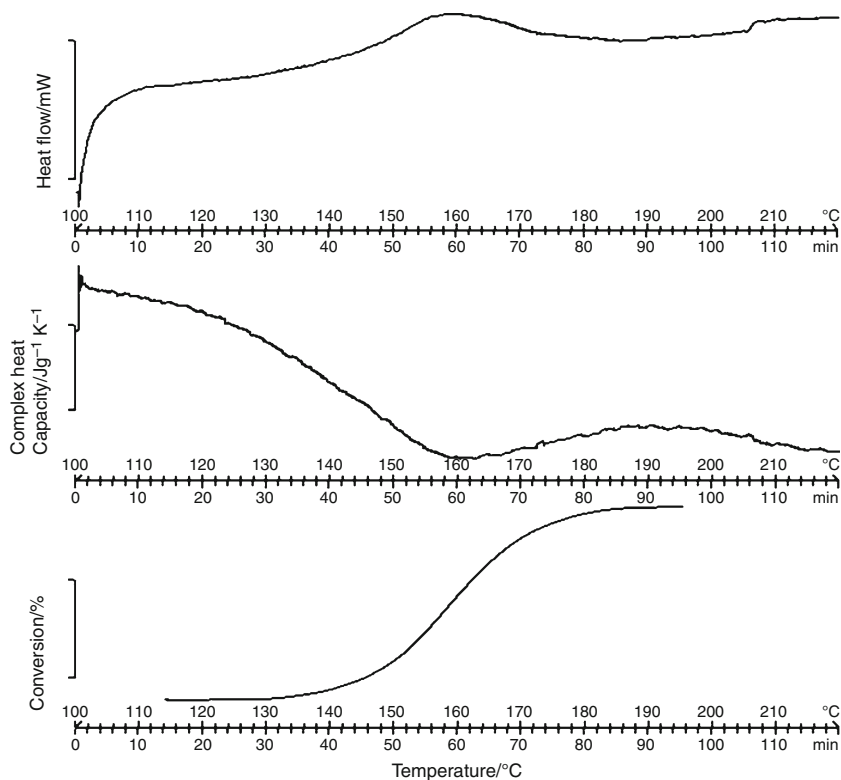
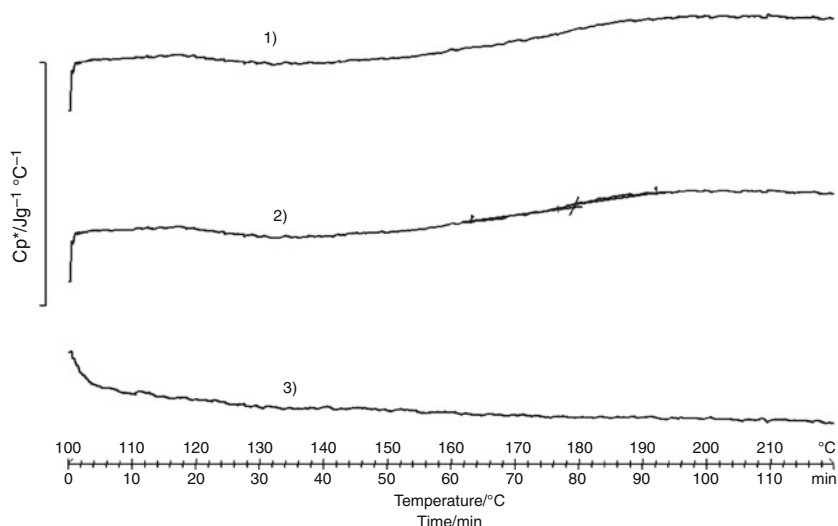


Fig. 3 (1) In-phase heat capacity, (2) modulus of complex heat capacity with the glass transition at about 176 °C, and (3) out of phase heat capacity of the fully cured epoxidized linseed oil



Isoconversional kinetic analysis

The calculated activation energy E_α dependence on conversion α using three different iso-conversional methods for the curing of epoxidized linseed oil with anhydride hardener are shown in Fig. 4. It is observed, that the KAS method shows a gradual decrease in activation energy at the initial stage of the cure before it remains constant until 40% conversion; with increasing conversion ($\alpha \geq 40\%$) again a decrease in activation energy is observed. Evident from Fig. 4 is also the very similar dependence of E_α on conversion of the FR- and VA-approaches. The KAS method yields a similar trend in E_α as calculated with the two other methods for conversions $\alpha \geq 40\%$; however, the changes in the absolute values of the activation energy at higher conversions are smaller and a stronger decrease in activation energy is only calculated for the final stage of cross-linking. These deviations in the activation energy versus conversion profiles among the various MFK

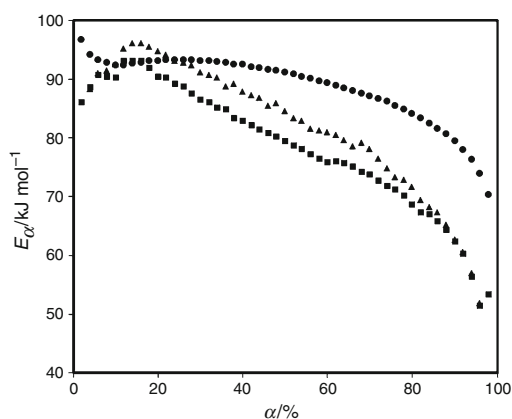


Fig. 4 Dependence of activation energy on conversion for the curing of epoxidized linseed oil using three different isoconversional methods (filled triangle FR, filled circle KAS, filled square VA)

methods are the result of the different mathematical approximations used by these methods [38].

The increase and decrease in the activation energy regime shows the complexity and also the molecular weight dependence of the epoxidized linseed oil cure. Park et al. [21] describe that the cross-linking of epoxies with anhydrides initially mainly proceeds via esterification while in the beginning of cure etherification plays no significant role. It is only in the later stages during cross-linking that etherification starts to contribute significantly to the overall curing mechanism until the final cross-linked network has reached gelation. Hence, in the studied epoxy-anhydride-imidazole system, the observed changes in activation energy at the initial stage of cure at around 18% conversion might be explained by a gradual shift in the relative importance of the contributions of esterification and etherification pathways.

Except for chemical changes in terms of new bond formation and an increase in molecular weight, there are also physical changes taking place during cure such as the development of mechanical properties. At an early stage, the reaction medium is liquid and is mainly composed of co-monomers and oligomers. As the reaction proceeds, the molecular weight of the forming polymer increases and due to this viscosity and the glass transition temperature increase as well. Since molecular mobility is strongly associated with the degree of cross-linking of the polymer chains, it decreases once network formation occurs until the cross-linked network has restricted molecular mobility so much that the resin changes from the liquid to the solid state, which can be either rubbery or glassy (if there is any vitrification). As seen from the E_α -profiles calculated by the VA and FR approaches (Fig. 4), the activation energy drops from initially 95 to 50 kJ mol⁻¹ in the end. This decrease in activation energy above 18% conversion can be explained by an increasing diffusion control of the curing

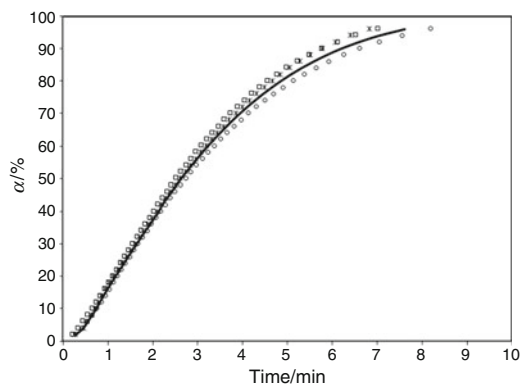


Fig. 5 Comparison of experimental degree of cure according to time with the Friedman, KAS, Vyazovkin predictions for isothermal curing at 180 °C (open circle KAS, open square Vyazovkin, open diamond Friedman, continuous line isothermal at 180 °C)

that is associated with vitrification [23]. In an earlier study by Sbirrazzuoli et al. [44] on the curing kinetics of the diglycidyl ether of bisphenol A (DGEBA) with *m*-phenylenediamine (*m*-PDA), the decrease in activation energy was also explained by a shift of the rate determining step from a kinetic to a diffusion controlled regime. The diffusion control was associated with the processes of gelation and vitrification that occur on curing and cause a dramatic decrease in molecular mobility.

In order to validate the kinetic models, an experimentally measured conversion versus time profile for an arbitrary isothermal temperature (at 180 °C) was compared with the calculated corresponding conversion versus time profiles as predicted by the three E_α curves at the same isothermal temperature (Fig. 5). The isothermal curing temperature of 180 °C was chosen above the $T_{g\infty}$ to avoid the effect of vitrification. It was found that, the FR and VA methods provide more consistent and accurate E_α functions than does the KAS method. The curing time predicted by the KAS method is lower as compared to the experimental value whereas minor deviations in the opposite direction were observed with both the FR and VA methods (Fig. 5). Among the three methods VA method is closer to the measured value although all three models predicted the actual curing reaction very well at the initial stage of cross-linking below 40% conversion.

Rheological behavior

The rheological behavior of the linseed oil resin changes with respect to time and temperature. Gelation and vitrification are the two major physical transformations that occur during cure and both can be monitored using rheological measurements.

Gelation is the physical transformation that occurs during cure once the average molecular weight reaches

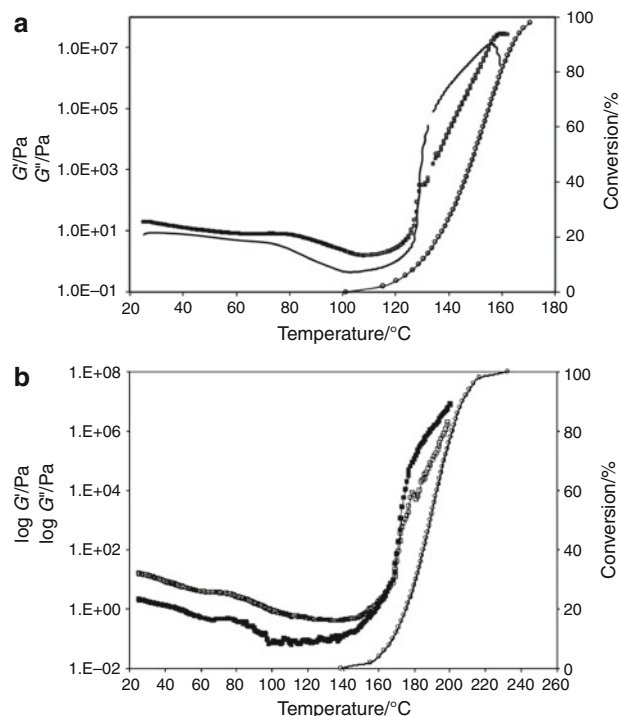


Fig. 6 The temperature dependence of loss and storage modulus in logarithmic scale for the epoxidized linseed oil measured with parallel plate rheometer at two different heating rates: **a** 1 °C min⁻¹ and **b** 10 °C min⁻¹ in comparison with cure conversion α calculated from dynamic DSC measurement at the same heating rate (filled square storage modulus G' , open square loss modulus G'' , open circle complex viscosity)

infinity. In contrast to vitrification, gelation does not usually inhibit the curing process and hence the rate of conversion typically remains unchanged. The rheological behavior during non-isothermal curing of the epoxidized linseed oil was studied using a parallel plate rheometer at two different heating rates 1 °C min⁻¹ (Figs. 6a, 7a) and 10 °C min⁻¹ (Figs. 6b, 7b). As discussed earlier, if the heating rate during non-isothermal cure is chosen high enough, then with an increase in curing temperature the increasing glass transition temperature T_g is always below the curing temperature and vitrification is avoided. The rheological data for two heating rates (1 and 10 °C min⁻¹) are depicted in Fig. 6. Considering the temperature range from 25 to 40 °C (Fig. 6a) and the temperature range from 25 to 60 °C (Fig. 6b, respectively), which represents a stage prior to the actual curing reaction, it is seen that the loss moduli G'' in both cases are higher than the storage moduli G' , which means that viscous effects dominate the system before the cross-linking starts. With further increasing temperature, the values of G'' decrease although they are always larger than the values of G' (see Fig. 6a, temperature range from 40 to 80 °C and Fig. 6b, respectively, temperature range from 60 to 100 °C).

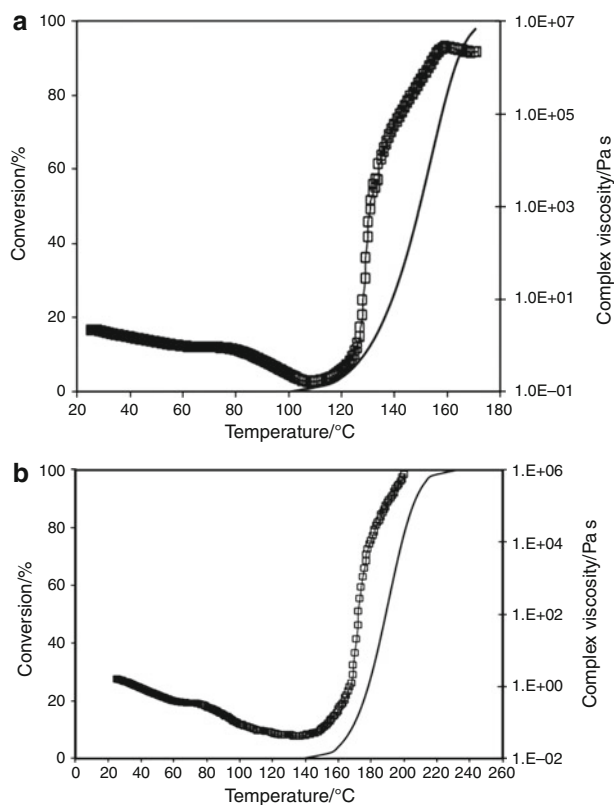


Fig. 7 The temperature dependence of complex viscosity in logarithmic scale for the epoxidized linseed oil measured with parallel plate rheometer at two different heating rates **a** $1\text{ }^{\circ}\text{C min}^{-1}$ and **b** $10\text{ }^{\circ}\text{C min}^{-1}$ in comparison with cure conversion α calculated from dynamic DSC measurement at the same heating rate (*Open square* complex viscosity [η^*], *continuous line* conversion α)

At the gelation point, the network structure changes from a sol to a gel state and from this stage on, the network structure begins to expand, and the sample transforms from a viscous substance into a visco-elastic material. This transformation is observed in the temperature region from 80 to 120 $^{\circ}\text{C}$ in Fig. 6a for the low heating rate and in the temperature region from 100 to 170 $^{\circ}\text{C}$ for the high heating rate. The gelation point is identified in the plot of G' and G'' versus temperature, where the viscous modulus equals the elastic modulus [45–47]. In the present ELO-NMA-1-MI system, gelation occurs at a conversion of ca. 18% which is independent of the applied heating rate (as evident from comparison of Fig. 6a, b). This value also corresponds to the significant maximum in E_a observed for the activation energy-versus-conversion plot obtained from the MFK analysis discussed in the previous section (Fig. 4).

After gelation, a state has been reached, where the reactants cannot anymore move freely and molecular mobility decreases further with an increase in temperature. This is reflected by the rapid increases in both viscous and storage modulus which were observed at conversions larger

than 18% in Fig. 6a and b. At this stage, there is no viscous flow anymore and the system transforms to either a rubbery or a solid state. In Fig. 6a the gel structure has changed into a glassy structure due to the vitrification effect which is observed by the substantial increase in the storage modulus and a maximum in the loss modulus, similar to the study by de la Caba et al. [48]. For the present ELO-NMA-1-MI system this phenomenon is observed in the temperature region between 125 and 160 $^{\circ}\text{C}$; it means that the system arrives at vitrification long before completion of the reaction when a low heating rate is employed for the curing. Vitrification is reversible upon further heating and hence, at temperatures $>160\text{ }^{\circ}\text{C}$ devitrification of the partially cured resin occurs, which is visible by the decrease in the storage modulus at these high temperatures in Fig. 6a. These findings are in good agreement with the ADSC data at the same low heating rate (compare Fig. 2) where at temperatures $>160\text{ }^{\circ}\text{C}$ a devitrification effect is observed.

In Fig. 6b, which summarizes the rheological behavior at a heating rate of $10\text{ }^{\circ}\text{C min}^{-1}$, there is no sign of vitrification, which can be proven by comparison of the modulus values at the different heating rates. At the same level of conversion (30% conversion), both modulus values for the heating rate $1\text{ }^{\circ}\text{C min}^{-1}$ ($G' = 7.6 \times 10^5$ and $G'' = 3.2 \times 10^4$) are comparatively higher than those obtained when a much higher heating rate of $10\text{ }^{\circ}\text{C min}^{-1}$ was applied ($G' = 1.1 \times 10^5$ and $G'' = 7.3 \times 10^3$). Above the gel point, the sample in Fig. 6a transforms into a glassy state which is observed by the very high modulus whereas the sample in Fig. 6b transforms into a rubbery state with a significantly lower modulus.

The complex viscosity (see Fig. 7a, b) runs through a minimum of 159 mPa s for the heating rate of $1\text{ }^{\circ}\text{C min}^{-1}$ and 4 mPa s for the heating rate $10\text{ }^{\circ}\text{C min}^{-1}$, respectively, before the actual start of the curing reaction. After gelation, the molecular weight reaches infinity and complex viscosity increases with an increase in temperature and conversion, which is also evident from Fig. 7. These rheological data can also be used to interpret the findings regarding the activation energy profiles described in the previous section. According to Sbirrazzouli et al. [49], viscous relaxation causes the initial difference in the E_x dependencies and at the stage where viscosity increases after a certain degree of conversion, the activation energy decreases due to a restricted molecular mobility. The conversion dependence of complex viscosity is related to a change in molecular mass and network development, so for the step growth polymerization the molecular mass of the polymer chains increases gradually. The gradual increase in complex viscosity with respect to conversion is observed in Fig. 7a and b. In Fig. 7a, the rapid non-linear increase in complex viscosity is observed from the onset of

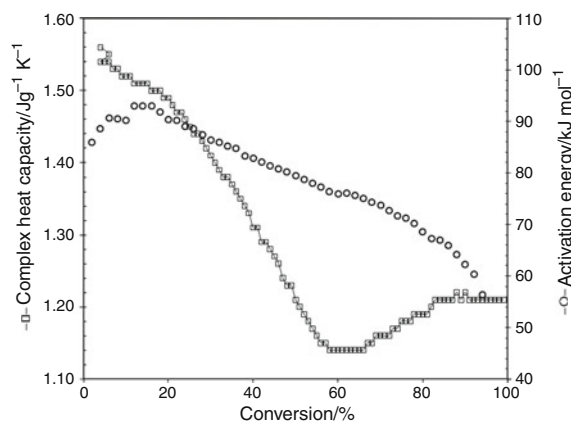


Fig. 8 The change in apparent activation energy calculated using Vyazovkin method are compared with the complex heat capacity measured using ADSC for the epoxidized linseed oil (*open square* complex heat capacity C_p^* , *open circle* activation energy)

vitrification at 18% conversion and this non-linear increase occurs up to conversions of 60%. The onset of vitrification is the same as the result predicted using ADSC measurements for the same heating rate $1\text{ }^\circ\text{C min}^{-1}$ (Fig. 2). At the low heating rate, T_g approaches the glass transition temperature of the fully cured network $T_{g\infty}$. Hence, the rate of reaction and the rate of the increase in T_g will drop further allowing the reaction temperature to surpass the T_g , which results in devitrification above 60% conversion. During devitrification, the non-isothermal transformation from a glassy state into a liquid or a rubbery state will occur, which is observed by the constant complex viscosity in Fig. 7a at conversions $>60\%$. The vitrification and devitrification effects are not observed for the measurement at heating rate of $10\text{ }^\circ\text{C min}^{-1}$, the samples gel but do not vitrify and instead undergo transition into a rubbery state.

In Fig. 8, the changes in apparent activation energy as calculated by the VA method are compared with changes in the complex heat capacity as measured by ADSC at a heating rate of $1\text{ }^\circ\text{C min}^{-1}$. In Fig. 8, at conversions above the gel point at $\alpha = 18\%$, the transition from the gel to the glassy state caused by vitrification is observed by the drastic decrease in complex heat capacity (until a conversion of $\alpha \approx 60\%$) and a concomitant decrease in the activation energy in this range from 95 to 75 kJ mol^{-1} , which is indicative of diffusion control in the cure system.

The dramatic decrease in molecular mobility causes a drop in complex heat capacity and due to this the activation energy values also decreased in the region of 20 to 60% conversion. The increase in complex heat capacity above 60% conversion corresponds to devitrification. Due to the restricted molecular mobility after reaching the gel point the activation energy drops irrespective of the heating rate.

Conclusions

The cure kinetics of an epoxidized linseed oil with an anhydride hardener was analyzed by the Friedman (FR), Kissinger–Akahira–Sunose (KAS) and Vyazovkin (VA) iso-conversional methods. The FR and VA methods provided consistent apparent activation energy for the complex epoxy curing. The complicated curing mechanism was well predicted by the model free kinetic methods and provided insight into the cure mechanism of epoxidized linseed oil with the anhydride hardener. The validation experiments showed that the VA method predicted more precisely the experimental values as did the other two methods. At the initial stage of conversion (α), an increase in activation energy was observed which might be due to the slow initiation mechanism. Gelation occurred at around 18% conversion and was determined quantitatively from rheological measurements. Once after initiation, during propagation (after gelation), a decrease in activation energy was observed, which was due to the transition from chemical to diffusion controlled process regardless of the heating rate. But at the lower heating rate the diffusion controlled process was predominantly influenced by the chemo-rheological effect called vitrification, which was observed by the abrupt decrease in complex heat capacity. The effect of vitrification was visible in rheological measurements where at the same degree of conversion the viscosity for the vitrified medium was higher than for the non-vitrified medium. During the non-isothermal cure the vitrification was followed by devitrification identified using ADSC measurement.

References

- Griffin Shay E. Diesel fuel from vegetable oils: status and opportunities. *Biomass Bioenergy*. 1993;4(4):227–42.
- Hill K. Fats and oils as oleochemical raw materials. *Pure Appl Chem*. 2000;72:1255–64.
- Daniel G, Farminer KW, Narayan R, Tran PT. Triglyceride based lubricant, US Patent 7601677 (2004).
- Paster M, Pellegrino JL, Carole TM. Industrial bio-products: today and tomorrow. <http://www.bioproducts-bioenergy.gov/pdfs/BioProductsOpportunitiesReportFinal.pdf> (2003).
- Meffert A, Kluth H. Process for the preparation of modified triglycerides. US Patent 4886893 (1989).
- Klaas MRG, Warwel S. Lipase-catalyzed preparation of peroxy acids and their use for epoxidation. *J Mol Catal A*. 1997; 117(1–3):311–9.
- Hill K. Fats and oils as oleo-chemical raw materials. *Pure Appl Chem*. 2000;72(7):1255–64.
- Mahendran AR, Aust N, Wuzella G, Kandelbauer A. Synthesis and characterization of biobased resin from linseed oil. *Macromolecular Symposia* (in press).
- Boquillon N, Fringent C. Polymer networks derived from curing of epoxidised linseed oil: influence of different catalysts and anhydride hardeners. *Polymer*. 2000;41:8603–13.

10. Zhu J, Chandrashekhara K, Flanigan V, Kapila S. Curing and mechanical characterization of a soy-based epoxy resin system. *J Appl Polym Sci.* 2004;91(6):3513–8.
11. Thames SF, Yu H. Ultraviolet-curable epoxidized sunflower oil/organoclay nanocomposite coatings. *Surf Coat Technol.* 1999; 115:208–14.
12. Park SJ, Jin FL, Lee JR. Thermomechanical behavior of epoxy resins modified with epoxidized vegetable oils. *Macromol Rapid Commun.* 2004;25:724–7.
13. Park SJ, Jin FL, Lee JR, Shin JS. Cationic polymerization and physicochemical properties of a biobased epoxy resin initiated by thermally latent catalysts. *Eur Polym J.* 2005;41:231–7.
14. Warth H, Müllhaupt R, Hoffmann B, Lawson S. Polyester networks based upon epoxidized and maleinated natural oils. *Angew Makromol Chem.* 1997;249(1):79–92.
15. Boquillon N. Use of an epoxidized oil-based resin as matrix in vegetable fibers-reinforced composites. *J Appl Polym Sci.* 2006; 101(6):4037–43.
16. Matejka L, Lovy J, Porkorny S, Bouchal K, Dusek K. Curing epoxy resins with anhydrides. Model reactions and reaction mechanism. *J Polym Sci Polym Chem Ed.* 1983;21:2873–85.
17. Brydson JA. *Plastic materials*, 7th edn. Boston: Butterworth-Heinemann; 2000. p. 760.
18. Alonso MV, Olliet M, Garcia J, Rodriguez F, Echeverria J. Gelation and isoconversional kinetic analysis of lignin–phenol–formaldehyde resin cure. *Chem Eng J.* 2006;122:159–66.
19. Berger J, Lohse F. Polymerization of p-cresyl glycidyl ether catalyzed by imidazoles. *Polym Bull.* 1984;12:535–42.
20. Berger J, Lohse F. Polymerization of p-cresyl glycidyl ether catalyzed by imidazoles I. The influence of the imidazole concentration, the reaction temperature, and the presence of isopropanol on the polymerization. *J Appl Polym Sci.* 1985;30:531–46.
21. Park WH, Lee JK, Kwon KJ. Cure behavior of an epoxy-anhydride imidazole system. *Polym J.* 1996;28(5):407–11.
22. Lange J, Altmann N, Kelly CT, Halley PJ. Understanding vitrification during cure of epoxy resins using dynamic scanning calorimetry and rheological techniques. *Polymer.* 2000;41(5): 5949–55.
23. Vyazovkin S, Sbirrazzuoli N. Isoconversional kinetic analysis of thermally stimulated processes in polymers. *Macromol Rapid Commun.* 2006;27:1515–32.
24. van Mele B, van Assche G, van Hemelrijck A. Modulated differential scanning calorimetry to study reacting polymer systems. *J Reinf Plast Comp.* 1999;18(10):885–94.
25. Kolar F, Svitilova J. Kinetics and mechanism of curing epoxy/anhydride systems. *Acta Geodyn Geom.* 2007;3(147):72–85.
26. Ivankovic M, Incarnato L, Kenny JM, Nicolai L. Curing kinetics and chemorheology of epoxy/anhydride system. *J Appl Polym Sci.* 2003;90(11):3012–9.
27. Ghaemy M, Riahy MH. Kinetics of anhydride and polyamide curing of bisphenol A-based diglycidyl ether using DSC. *Eur Polym J.* 1996;32(10):1207–12.
28. Vyazovkin S, Sbirrazzuoli N. Kinetic methods to study isothermal and nonisothermal epoxy-anhydride cure. *Macromol Chem Phys.* 1999;200(10):2294–303.
29. Brown ME, editor. *Handbook of thermal analysis and calorimetry*. Vol. 1: principles and practice, chap 3. Amsterdam: Elsevier Science, BV; 1998.
30. Wuzella G, Kandelbauer A, Mahendran AR, Teischinger A. Thermochemical and isoconversional kinetic analysis of a polyester–epoxy hybrid powder coating resin for wood based panel finishing. *Prog Org Coat.* 2011;70(4):186–91.
31. Friedman HL. Kinetics of thermal degradation of char-forming plastics from thermogravimetry, application to a phenolic plastic. *J Polym Sci.* 1964;C6(6):183–95.
32. Kissinger HE. Reaction kinetics in differential thermal analysis. *Anal Chem.* 1957;29(11):1702–6.
33. Akahira T, Sunose T. Res. Report Chiba Inst Technol. (Sci Technol). 1971;16:22–31.
34. Vyazovkin S. Evaluation of activation energy of thermally stimulated solid-state reactions under arbitrary variation of temperature. *J Comput Chem.* 1997;18(3):393–402.
35. Vyazovkin S. Modification of the integral isoconversional method to account for variation in the activation energy. *J Comput Chem.* 2001;22(2):178–83.
36. Vyazovkin S. Isoconversional kinetics. In: Brown ME, Gallagher PK, editors. *The handbook of thermal analysis & calorimetry*. Vol 5: recent advances, techniques and applications. New York: Elsevier; 2008. p. 503–38.
37. Kandelbauer A, Wuzella G, Mahendran A, Taudes I, Widsten P. Model-free kinetic analysis of melamine-formaldehyde resin cure. *Chem Eng J.* 2009;152(2–3):556–65.
38. Vyazovkin S. A unified approach to kinetic processing of non-isothermal data. *Int J Chem Kinet.* 1996;28(2):95–101.
39. Polijansek I, Krajnc M. Alternating differential scanning calorimetry: isothermal curing of the epoxy resin. *Acta Chim Slov.* 2003;50:461–72.
40. Simon SL. Temperature-modulated differential scanning calorimetry: theory and application. *Thermochim Acta.* 2001;374: 55–71.
41. Reading M, Douglas JS. *Modulated temperature differential scanning calorimetry*, vol 6. New York: Springer; 2006.
42. Montserrat S, Calventus Y, Colomer P. Vitrification and devitrification phenomena in the dynamic curing of an epoxy resin with ADSC. *Usercom 1/2000*, Mettler Toledo. 2000;17–19.
43. Montserrat S, Martin JG. Non-isothermal curing of a diepoxide–cycloaliphatic diamine system by temperature modulated differential scanning calorimetry. *Thermochim Acta.* 2002;388:343–54.
44. Sbirrazzuoli N, Vyazovkin S, Mititelu A, Sladic C, Vincent L. A study of epoxy-amine cure kinetics by combining isoconversional analysis with temperature modulated DSC and dynamic rheometry. *Macromol Chem Phys.* 2003;204(15):1815–21.
45. ASTM D 4473-85. *American Society for Testing and Materials*, New York; 1985. p 482.
46. Winter HH. Can the gel point of a cross-linking polymer be detected by the $G'–G''$ crossover? *Polym Eng Sci.* 1987;27:22.
47. Tung CYM, Dynes JP. Relationship between viscoelastic properties and gelation in thermosetting systems. *J Appl Polym Sci.* 1982;27(2):569–74.
48. de la Caba K, Guerrero P, Eceiza A, Mondragon I. Kinetic and rheological studies of an unsaturated polyester cured with different catalyst amounts. *Polymer.* 1996;37(2):275–80.
49. Sbirrazzuoli N, Vyazovkin S. Learning about epoxy cure mechanisms from isoconversional analysis of DSC data. *Thermochim Acta.* 2002;388:289–98.